Supplemental Information

DNA METHYLATION PREPROCESSING

DNA methylation (DNAm) preprocessing was conducted with the minfi package.[59] Before calculation of methylation profiles, CpG probes with detection $P > .05$ and <3 beads in >1% of the samples, probes in cross-reactive regions, and those containing a single-nucleotide polymorphism with minor allele frequency >0.01 within 10 base pairs of the single base extension position or at the CpG interrogation were excluded.[60] DNAm values were normalized with noob background correction as implemented by minfi's preprocessNoob function.[61] Eight participants were excluded for poor-performing probes: they showed low-intensity probes, as indicated by the log of average methylation <11, and their detection P was >.05 in >10% of their probes.

DNAm differs between cell tissue types; thus, it is important to residualize for cell composition. Cell composition was estimated in 2 ways. First, the blood-based FlowSorted.Blood.450k R package is used to estimate CD8 T cells, CD4 T cells, natural killer cells, B cells, monocytes, and granulocytes.[62] Second, we estimated 5 cell types using the tissue reference-free method by Houseman et al,[63] as implemented in the RefFreeCellMixArray R package. The association of DunedinPoAm-measured pace of aging residualized with the blood-based control and DunedinPoAm-measured pace of aging residualized with the reference-free method was strong (r = 0.97, 95% CI 0.95 to 0.99, $P <$ .001). We therefore report results of methylation profiles residualizing for cell composition using the blood-based estimation. DNAm profiles were also residualized for array and slide; all samples came from the same batch.

COMPARISON OF DUNEDINPOAM-MEASURED PACE OF AGING IN SALIVA AND BLOOD

DunedinPoAm was developed from an analysis of blood DNAm data. Texas Twin Project DNAm data were generated from saliva DNA samples. We conducted an analysis to evaluate the expected correspondence between the saliva DNAm DunedinPoAm-measured pace of aging values we analyzed in participants of the Texas Twin Project and DunedinPoAm-measured pace of aging values from blood. We analyzed Illumina EPIC array blood and saliva DNAm data sets derived from a set of 21 individuals published by Braun et al[64] (data were downloaded from the Gene Expression Omnibus, accession GSE111165). We measured DunedinPoAm pace of aging in these data, following the method described previously, using an R package available on GitHub (https://github.com/danbelsky/DunedinPoAm38)[24]. We used the DNA Methylation Age Calculator hosted by the Horvath Laboratory (http://dnamage.genetics.ucla.edu/) to compute estimates of leukocyte proportions in the data, along with the DNAmAge multi-tissue epigenetic clock developed by Horvath.[27] The analysis proceeded in 3 steps: First, we corrected all DNAm-based measures for the sample batch by calculating residual values from regressions of DNAm measures on batch identifiers. Second, we computed cell-count residuals of batch-corrected DunedinPoAm-measured pace of aging by regressing DunedinPoAm values on estimates of CD8 T-cell, CD4 T-cell, natural killer–cell, B-cell, monocyte, and granulocyte proportions on the basis of the algorithms developed by Houseman et al[65] and plasma blasts, CD4 and CD8 naïve T cells, and memory T cells on the basis of algorithms developed by Horvath. For saliva measures, CD8 T cells were omitted from regressions because estimated proportions were near 0. Third, we computed the correlation between the cell-count residuals computed from blood and saliva DNAm data sets. Data are plotted in Supplemental Fig 3. Observations for which blood and saliva DNAm samples were run in the same batch are indicated in red. The cross-tissue correlation for these observations is r = 0.85. For the full data set, which includes an additional 7 observations for which the tissues were run in separate batches, the cross-tissue correlation is r = 0.60.

EPIGENETIC CLOCKS

We computed 5 epigenetic clocks. The original clocks proposed by Horvath[27] and by Hannum et al[26] were derived from DNAm analysis of

chronological age. The same approach was used to develop a pediatric clock optimized to predict the age of children from buccal cell DNAm (PedBE).[30] In addition to these 3 chronological age–based clocks, we analyzed 2 recently published clocks developed from DNAm analysis of mortality risk, PhenoAge[28] and GrimAge.[29] These clocks were developed in 2 steps. For the PhenoAge clock, the first step modeled mortality risk from chronological age and a panel of biomarkers in data from the US National Health and Nutrition Examination Surveys III data. In the second step, predicted risk derived from the first-step model was, in turn, modeled from DNAm data in the InCHIANTI cohort. For the GrimAge clock, in the first step, blood proteins were modeled from DNAm data in the Framingham Heart Study Offpsring Cohort. In the second step, mortality risk was modeld from DNAm estimates of blood proteins, a DNAm prediction of smoking history, chronological age, and sex in this same cohort. The PhenoAge and GrimAge clocks remain highly correlated with chronological age but are more strongly related to disease and mortality compared with the Horvath and Hannum clocks. The Horvath clock was developed from an analysis of multiple tissues. The Hannum clock and the PhenoAge and GrimAge clocks were developed from an analysis of blood DNAm data. The PedBE clock was developed from analysis of buccal cells.

Epigenetic clocks were computed by using the DNA Methylation Age Calculator hosted by the Horvath Laboratory (http://dnamage.genetics.ucla.edu/). Following standard methods, we converted clocks to age-acceleration residuals for analysis by regressing participants' computed epigenetic-clock age values on their chronological ages and predicting residual values.

RESULTS

Comparison of Results With Those of Epigenetic Clocks

We compared results for DunedinPoAm with results from an analysis of 5 published epigenetic clocks: (1) Horvath[27] DNAm age (before correction for the cell composition of saliva samples: mean = 14.96, SD = 4.38, 95% CI 14.61 to 15.31), (2) Hannum et al[26] DNAm age (before cell correction: mean = 22.57, SD = 3.46, 95% CI 22.29 to 22.84), (3) PedBE (before cell correction: mean = 11.04, SD = 1.98, 95% CI 10.88 to 11.19), (4) PhenoAge (before cell correction: mean = 17.26, SD = 5.53, 95% CI 16.82 to 17.70), and (5) GrimAge (before cell correction: mean = 35.84, SD = 3.33, 95% CI 35.58 to 36.11). All 5 epigenetic clocks were strongly correlated with chronological age (median $r = 0.74$; Supplemental Fig 4A).

For analysis, we regressed clock values on children's chronological age to compute age-acceleration residuals. These residuals are interpreted as how much more or less aging has occurred in a person compared to the expectation based on their chronological age. DunedinPoAm was moderately correlated with the PhenoAge and GrimAge clock residuals (PhenoAge: $r = 0.21$; GrimAge: $r = 0.29$) and weakly correlated with the Horvath[27] and Hannum et al[26] clock residuals (Horvath[27]: $r = 0.09$; Hannum et al[26]: $r = 0.07$). Correlations are reported in Supplemental Fig 4B.

We repeated the analysis of socioeconomic disadvantage, replacing DunedinPoAm with each of the epigenetic-clock residuals in turn. In contrast to results for DunedinPoAm, epigenetic clocks were not associated with socioeconomic disadvantage and, in 2 cases, associations were in the opposite direction expected (range of $r = -0.03$ to 0.05; Table 1).

Comparison of Results for 1 Twin and Clustered SEs

To ensure that our primary mixed-effects models appropriately corrected for nonindependence of the sample, we reran models with 1 randomly selected twin per pair and also reran models with clustered SEs in Mplus software.[66] The coefficients were similar across all analytic strategies, increasing confidence in the robustness of our results (Supplemental Table 3).

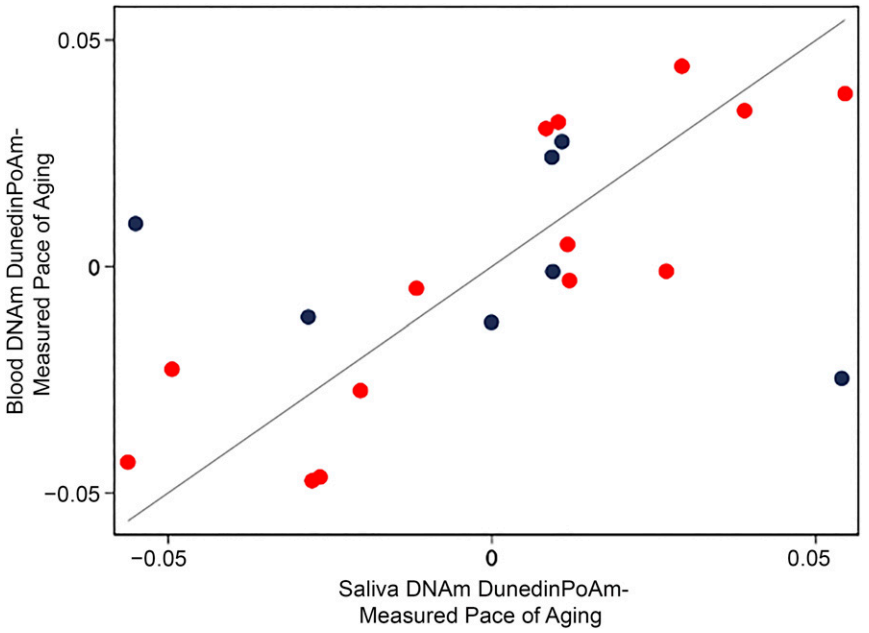

SUPPLEMENTAL FIGURE 3

Blood-to-saliva cross-tissue correlation of the DunedinPoAm measure in the Gene Expression Omnibus data set GSE111165 published by Braun et al.[64] The figure plots DunedinPoAm-measured pace of aging values in blood on the y-axis against DunedinPoAm-measured pace of aging values in saliva on the x-axis. The gray line illustrates perfect correspondence. Observations for which blood and saliva DNAm were run in the same batch are indicated in red. The cross-tissue correlation for these observations is $r = 0.85$. For the full data set, which includes an additional 7 observations for which the tissues were run in separate batches, the cross-tissue correlation is $r = 0.6$.

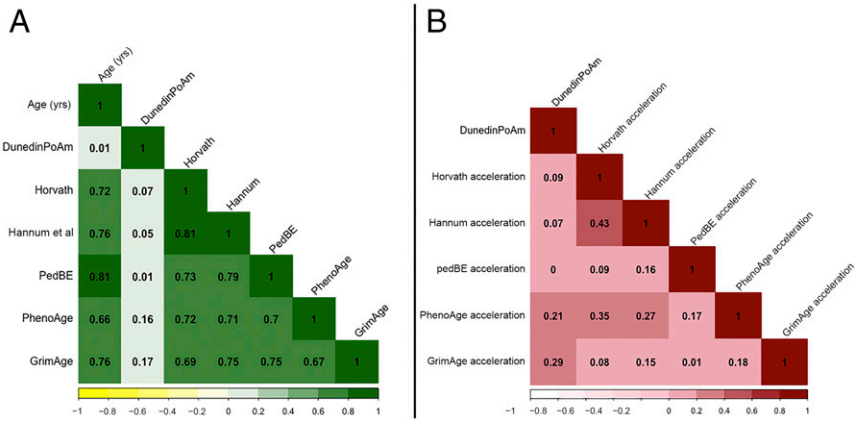

SUPPLEMENTAL FIGURE 4

Correlations among DunedinPoAm and 5 epigenetic clocks. A, The correlation matrix of the methylation pace of aging (DunedinPoAm) and epigenetic-age clocks with chronological age after residualizing for array, slide, and cell composition. B, The correlation matrix of the methylation pace of aging (DunedinPoAm) and epigenetic-age acceleration after residualizing for chronological age, array, slide, and cell composition.

SUPPLEMENTAL TABLE 3 Associations Between Socioeconomic Disadvantage and DunedinPoAm-Measured Pace of Aging in Primary Mixed-Effects Models, Models With One Randomly Selected Twin, and Models With Clustered SEs in Mplus

	Family-Level Socioeconomic Disadvantage			Neighborhood-Level Socioeconomic Disadvantage		
	r	95% CI	*P*	*r*	95% CI	*P*
Primary mixed-effects models	0.18	0.08 to 0.27	.001	0.18	0.07 to 0.28	.001
Mixed-effects models with 1 twin	0.24	0.13 to 0.35	<.001	0.18	0.07 to 0.29	.002
Models with clustered SEs in Mplus	0.17	0.07 to 0.27	.001	0.17	0.07 to 0.27	.001

Standardized regression coefficients (*r*) and 95% CIs were calculated by regressing DunedinPoAm-measured pace of aging on family-level socioeconomic disadvantage and neighborhood-level socioeconomic disadvantage separately. All models included covariate adjustment for the child's age and sex.

SUPPLEMENTAL REFERENCES

59. Aryee MJ, Jaffe AE, Corrada-Bravo H, et al. Minfi: a flexible and comprehensive Bioconductor package for the analysis of Infinium DNA methylation microarrays. *Bioinformatics*. 2014;30(10):1363–1369
60. Pidsley R, Zotenko E, Peters TJ, et al. Critical evaluation of the Illumina MethylationEPIC BeadChip microarray for whole-genome DNA methylation profiling. *Genome Biol*. 2016;17(1):208
61. Triche TJ Jr, Weisenberger DJ, Van Den Berg D, Laird PW, Siegmund KD. Low-level processing of Illumina Infinium DNA Methylation BeadArrays. *Nucleic Acids Res*. 2013;41(7):e90
62. Jaffe AE. *FlowSorted.Blood.450k: Illumina HumanMethylation data on sorted blood cell populations [computer program] 2020. R package version 1.28.0*
63. Houseman EA, Kile ML, Christiani DC, Ince TA, Kelsey KT, Marsit CJ. Reference-free deconvolution of DNA methylation data and mediation by cell composition effects. *BMC Bioinformatics*. 2016;17:259
64. Braun PR, Han S, Hing B, et al. Genome-wide DNA methylation comparison between live human brain and peripheral tissues within individuals. *Transl Psychiatry*. 2019;9(1):47
65. Houseman EA, Accomando WP, Koestler DC, et al. DNA methylation arrays as surrogate measures of cell mixture distribution. *BMC Bioinformatics*. 2012; 13:86
66. Muthén LK, Muthén BO. *Mplus User's Guide*. 8th ed. Los Angeles, CA: Muthén & Muthén; 2017